Phytochemistry 169 (2020) 112163

Contents lists available at ScienceDirect

Phytochemistry

journal homepage: www.elsevier.com/locate/phytochem

Identification, characterization, and antifungal activity of cysteine peptidases from *Calotropis procera* latex

Cleverson D.T. Freitas[a,*], Rafaela O. Silva[a], Márcio V. Ramos[a], Camila T.M.N. Porfírio[a], Davi F. Farias[b], Jeanlex S. Sousa[c], João P.B. Oliveira[a], Pedro F.N. Souza[a], Lucas P. Dias[a], Thalles B. Grangeiro[d]

[a] Departamento de Bioquímica e Biologia Molecular, Universidade Federal do Ceará, Centro de Ciências, Campus do Pici, Fortaleza, Ceará, CEP, 60440-900, Brazil
[b] Departamento de Biologia Molecular, Universidade Federal da Paraíba, Campus I, CEP, 58051-900, João Pessoa, Brazil
[c] Departamento de Física, Universidade Federal do Ceará, Fortaleza, Brazil
[d] Departamento de Biologia, Universidade Federal do Ceará, Fortaleza, Brazil

ARTICLE INFO

Keywords:
Calotropis procera (Aiton) Dryand (Apocynaceae)
Latex
Oxidative stress
Phytopathogens
Plant defense
Protease

ABSTRACT

Cysteine peptidases (EC 3.4.22) are the most abundant enzymes in latex fluids. However, their physiological functions are still poorly understood, mainly related to defense against phytopathogens. The present study reports the cDNA cloning and sequencing of five undescribed cysteine peptidases from *Calotropis procera* (Aiton) Dryand (Apocynaceae) as well as some in silico analyses. Of these, three cysteine peptidases (CpCP1, CpCP2, and CpCP3) were purified. Their enzymatic kinetics were determined and they were assayed for their efficacy in inhibiting the hyphal growth of phytopathogenic fungi. The mechanism of action was investigated by fluorescence and atomic force microscopy as well as by induction of reactive oxygen species (ROS). The deduced amino acid sequences showed similar biochemical characteristics and high sequence homology with several other papain-like cysteine peptidases. Three-dimensional models showed two typical cysteine peptidase domains (L and R domains), forming a "V-shaped" active site containing the catalytic triad (Cys, His, and Asn). Proteolysis of CpCP1 was higher at pH 7.0, whereas for CpCP2 and CpCP3 it was higher at 7.5. All peptidases exhibited optimum activity at 35 °C and followed Michaelis-Menten kinetics. However, the major difference among them was that CpCP1 exhibited highest V_{max}, K_m, K_{cat} and catalytic efficiency. All peptidases were deleterious to the two fungi tested, with IC_{50} of around 50 μg/mL. The peptidases promoted membrane permeabilization, morphological changes with leakage of cellular content, and induction of ROS in *F. oxysporum* spores. These results corroborate the hypothesis that latex cysteine peptidases play a role in defense against fungi.

1. Introduction

Peptidases are among the most studied enzymes because they are involved in several physiological processes responsible for the homeostasis of living organisms. In plants, peptidases can be involved in recognition and/or induction of defense responses against pathogens (Figueiredo et al., 2014) and insects (Meyer et al., 2016), abiotic stress tolerance (Chen et al., 2017), seed germination (Lu et al., 2015), pollen development (Zhang et al., 2014), senescence (Avila-Ospina et al., 2014), programmed cell death (Daneva et al., 2016), and protein turnover (Nelson and Millar, 2015), among others. This wide range of functions can explain, at least in part, the high number of peptidase genes in plant genomes. For instance, in the *Arabidopsis thaliana* and *Oryza sativa* genomes, more than 800 and 600 peptidase genes have been identified, respectively (van der Hoorn, 2008). Therefore, it is hypothesized that the expression and activity of each peptidase are coordinated and controlled as well as require specific stimuli (van Wijk, 2015; Hou et al., 2018).

Latex is the cytoplasm of living plant cells called laticifers, which are rich in peptidases (Ramos et al., 2019). More than 100 different plant families are known to contain at least one proteolytic enzyme, belonging mainly to the cysteine peptidase class (Domsalla and Melzig, 2008). Papain, a cysteine peptidase purified from *Carica papaya* latex, is the best known and studied plant proteolytic enzyme because of its many applications (Feijoo-Siota and Villa, 2011). Other latex fluids have also been targets of study, since they are also rich in peptidases (Freitas et al., 2007, 2010; 2016a; Oliveira et al., 2019a). In some laticifers, these enzymes can constitute up to 90% of all the latex proteins,

* Corresponding author.
E-mail addresses: cleversondiniz@ufc.br, cleversondiniz@hotmail.com (C.D.T. Freitas).

https://doi.org/10.1016/j.phytochem.2019.112163
Received 3 June 2019; Received in revised form 26 September 2019; Accepted 2 October 2019
Available online 09 October 2019
0031-9422/

as in *Ficus carica* (Zare et al., 2013), or be present in several isoforms, as in *Thevetia peruviana* latex, where 20 peptidases with different molecular masses and pI values have been identified (Freitas et al., 2016b). Although cysteine peptidases are widely distributed in latex fluids, their physiological functions are still poorly understood. Therefore, further research is needed to identify and characterize the biological activities of undescribed latex cysteine peptidases.

Calotropis procera, a plant from the Apocynaceae family, has been studied because its latex is rich in peptidases (Freitas et al., 2007). To date, five cysteine peptidases have been purified and partially characterized from it (procerain, procerain B, CpCP 1, CpCP 2, and CpCP 3). However, their physiological functions have not been investigated (Dubey and Jagannadham, 2003; Singh et al., 2010; Ramos et al., 2013). In addition, 20 cysteine peptidase genes from *C. procera* were sequenced by Kwon et al. (2015), but again their roles in plant defense were not examined. Finally, *C. procera* peptidases have exhibited diverse biotechnological applications, such as blood coagulation, with thrombin- and plasmin-like activities (Ramos et al., 2012), cheese making (Freitas et al., 2016a), dehairing of leather (Lopéz et al., 2017), and wound healing modulation (Ramos et al., 2016). Because of these diverse applications, *C. procera* peptidases have gained attention and studies have been performed to characterize them. Here, five undescribed cysteine peptidase genes from *C. procera* were identified, partially characterized, and the antifungal activities and action mechanism of three purified proteins were preliminarily evaluated against two phytopathogenic fungi.

2. Results

2.1. PCR, cDNA cloning and sequence analysis

Total RNA was extracted from *C. procera* leaves and used to obtain cDNAs encoding putative cysteine peptidases by 3' RACE-PCR. The amplified products using four degenerate primers (Cyspept 1, Cyspept 2, Cyspept 3, and Cyspept 4) were checked by 1% agarose gel electrophoresis and the best amplification results were obtained at an annealing temperature of 56 °C (Fig. S1). Fragments of approximately 784 (Cyspept 1), 837 (Cyspept 2), 667 (Cyspept3) and 694 pb (Cyspept 4) were isolated, cloned, and the presence of the inserts in different clones was confirmed by restriction digestion with *Eco*RI (Fig. S2), followed by sequencing. This analysis resulted in the identification of five cysteine peptidase sequences, which were named *Calotropis procera* Cysteine Peptidase A, B, C, D, and E (CpCP A, CpCP B, CpCP C, CpCP D, and CpCP E, respectively). All cDNA sequences were submitted to the GenBank database (Fig. S3) (GenBank accession numbers: CpCP A MN444884; CpCP B MN444885; CpCP C MN444886; CpCP D MN444887; CpCP E MN444888).

Some biochemical characteristics of cysteine peptidases, including molecular masses, isoelectric points (pI), numbers of cysteine residues, and disulfide bridges are shown in Table 1. The amino acid sequences exhibited high similarity with other plant cysteine peptidases, including the cysteine peptidases from *C. procera* and *Nicotiana sylvestris* (Table 1). However, they exhibited differences between each other and in relation to the other 22 cysteine peptidases from *C. procera*: procerain (AMY15659), procerain B (Singh et al., 2013), and SnuCalCp01-20 (Kwon et al., 2015) (Fig. 1 and Fig. S4). All cysteine peptidases from *C. procera*, which include CpCP A, CpCP B, CpCP C, CpCP D, CpCP E, procerain, procerain B, and SnuCalCp01-20, displayed the same conserved catalytic triad (cysteine, histidine and asparagine) and three disulfide bridges (Fig. 1), when compared to papain, suggesting these peptidases share common structures and enzymatic properties and belong to the peptidase C1A superfamily.

2.2. Molecular modeling

The biochemical characteristics, multiple sequence alignment and phylogenetic analysis of the five cysteine peptidases from *C. procera* showed that CpCP A was more similar to CpCP E (Group 1), while CpCP B and CpCP D (Group 2) were gathered in the same group. Even though classified in another group, CpCP C (Group 3) showed higher similarity with CpCP B and CpCP D (Fig. S4). Thus, the molecular modeling assays were performed using CpCP A, CpCP D and CpCP C to represent groups 1, 2 and 3, respectively.

Three-dimensional models were obtained by homology modeling using different cysteine peptidase structures (PDB number: 1BY8, 1NB5, 1IWD or 1S4V) as templates (Fig. 2). The quality of final models was validated by the Ramachandran plot, ERRAT2, ProSA, and Verify 3D servers, which revealed that the best models were those generated by the SWISS-MODEL platform (Table S1). The three 3D models presented two typical domains (L and R domains) of cysteine peptidases, forming a "V-shaped" active site containing the catalytic triad (Cys, His, Asn) (Figs. 1 and 2). The root means square deviation (RMSD) between the main chain atoms of CpCP A, CpCP C, and CpCP D and their respective templates (PDB numbers: 1BY8, 1NB5 and 1IWD, respectively) were obtained with values of 0.435 Å, 0.460 Å, and 0.381 Å, indicating that the generated models were well fitted.

2.3. Protein identification, enzymatic kinetics and antifungal assays

Considering that the five CpCP cDNA sequences were obtained from *C. procera* leaves, which are rich in laticifers, we hypothesized that these genes are expressed in the latex. To confirm this hypothesis, the three cysteine peptidases purified from *C. procera* latex (CpCP1, CpCP2 and CpCP3) were digested by trypsin, analyzed by mass spectrometry and the peptides were aligned with the five CpCP cDNA sequences (Fig. S5). The alignment showed that CpCP1, CpCP2, and CpCP3 were the mature proteins represented by CpCP A, CpCP E and CpCP C, respectively (Fig. S5).

The maximum proteolytic activity was achieved at pH 7.0 for CpCP1 and 7.5 for CpCP2 and CpCP3 (Fig. 3A). The three peptidases exhibited optimum activity at 35 °C and followed Michaelis-Menten kinetics (Fig. 3B and C). CpCP1 exhibited V_{max} and K_m of 65.89 ± 2.80 nkat and 1.27 ± 0.08 mM, whereas the V_{max} and K_m for CpCp2 and CpCP3 were 19.52 ± 0.65 nkat and 0.61 ± 0.04 mM, and 18.72 ± 2.11 nkat and 0.87 ± 0.17 mM, respectively (Fig. 3 C). K_{cat} values for CpCP1, CpCP2 and CpCP3 were 16.4 s^{-1}, 4.3 s^{-1} and 4.1 s^{-1}, respectively. The catalytic efficiency of CpCP1 (K_{cat}/K_m = 12,913 $M^{-1} s^{-1}$) was 1.8-fold higher than that of CpCP2 (K_{cat}/K_m = 7049 $M^{-1} s^{-1}$) and 2.7-fold higher than that of CpCP3 (K_{cat}/K_m = 4712 $M^{-1} s^{-1}$).

The effect of the three purified cysteine peptidases from *C. procera* latex (CpCP1, CpCP2 and CpCP3) on two phytopathogenic fungi, was investigated first by inhibition of growth. The three cysteine peptidases exhibited inhibitory activity with IC_{50} values of approximately 50 µg/mL for *F. oxysporum* and *C. acutatum* (Fig. 4) ($p > 0.05$). Because there was no statistical difference among the antifungal activities shown by three latex peptidases, we hypothesized that their antifungal action mechanisms were similar. Therefore, only one fungus (*F. oxysporum*) was used for further action mechanism assays. The action mechanism of latex peptidases was first evaluated by atomic force microscopy. The images showed that the three cysteine peptidases drastically altered the morphology and volume of *F. oxysporum* spores (Fig. 5, gray arrows) as well as caused a loss of internal content (Fig. 5, white arrows), when compared to the control spores, which had a smooth surface with no apparent damage or rupture.

Fig. 6 indicates that the three cysteine peptidases (CpCP1, CpCP2, and CpCP3, at 50 µg/mL, IC_{50}) induced membrane permeabilization in *F. oxysporum* spores, since fluorophore propidium iodide only penetrates cells with damaged plasma membranes. The red fluorescence observed is a consequence of DNA-dye binding. Intense fluorescence was also observed around the spores, corroborating the membrane damage and release of intracellular content shown by AFM (Fig. 5).

Table 1
Some theoretical characteristics obtained from amino acid sequences of five cysteine peptidases genes from *Calotropis procera*.

Peptidase	Protein length	Molecular mass*	Isoelectric point*	Cysteine residues*	Disulphide bridges (amino acids)**	BLASTP best match*** (Protein/Species/ Accession number)	Identity (E-Value)
CpCP A	225	24,820.78	4.2	8	3 (4–47; 38–80; 138–188)	Cysteine proteinase [*Nicotiana sylvestris*] XP_009800592.1	76% ($2e^{-110}$)
CpCP B	194	21,614.41	8.9	7	3 (4–45; 38-77; 132–183)	Procerain [*Calotropis procera*] AMY15659.1	84% ($1e^{-106}$)
CpCP C	197	21,726.64	9.2	7	3 (4–45; 38-77; 132–184)	Procerain [*Calotropis procera*] AMY15659.1	78% ($1e^{-96}$)
CpCP D	194	21,542.34	9.1	7	3 (4–45; 38-77; 132–183)	Procerain [*Calotropis procera*] AMY15659.1	85% ($1e^{-107}$)
CpCP E	200	21,979.43	4.1	8	3 (4–47; 38-80; 138–188)	Cysteine proteinase [*Nicotiana sylvestris*] XP_009800592.1	75% ($3e^{-108}$)

* The EMBOSS Pepstats server was used to compute the theoretical molecular mass, isoelectric point and cysteine residues (http://www.bioinformatics.nl/emboss-explorer/).
** The DiANNA 1.1 web server was used to predict the disulfide bonds (http://clavius.bc.edu/~clotelab/DiANNA/).
*** The BLASTP was used to compare the protein query sequence against a protein sequence database in NCBI (https://blast.ncbi.nlm.nih.gov/Blast.cgi?PAGE=Proteins).

Although the fluorophore propidium iodide indicates damage to the membrane, it does not give any further information about the pore size or membrane damage. To fill that gap, spores treated with CpCP1, CpCP2, and CpCP3 were incubated with three FITC-conjugated molecules with known molecular sizes [6000 Da (Calcein), 20,000 Da (FT-20), and 30,000 Da (FT-30)]. After analysis, fluorescence was not detected neither in the control spores non those treated with CpCP1, CpCP2, and CpCP3 (data not shown), suggesting peptidases did not form pores or the pores had exclusion size > 6000 Da.

The induction of reactive oxygen species (ROS) was also examined in spores treated with CpCP1, CpCP2 and CpCP3, since their overproduction can lead to cell death by apoptosis or necrosis, resulting in leakage of internal cell contents. Fig. 7 shows low or negligible ROS production in the control spores, whereas in the peptidase-treated

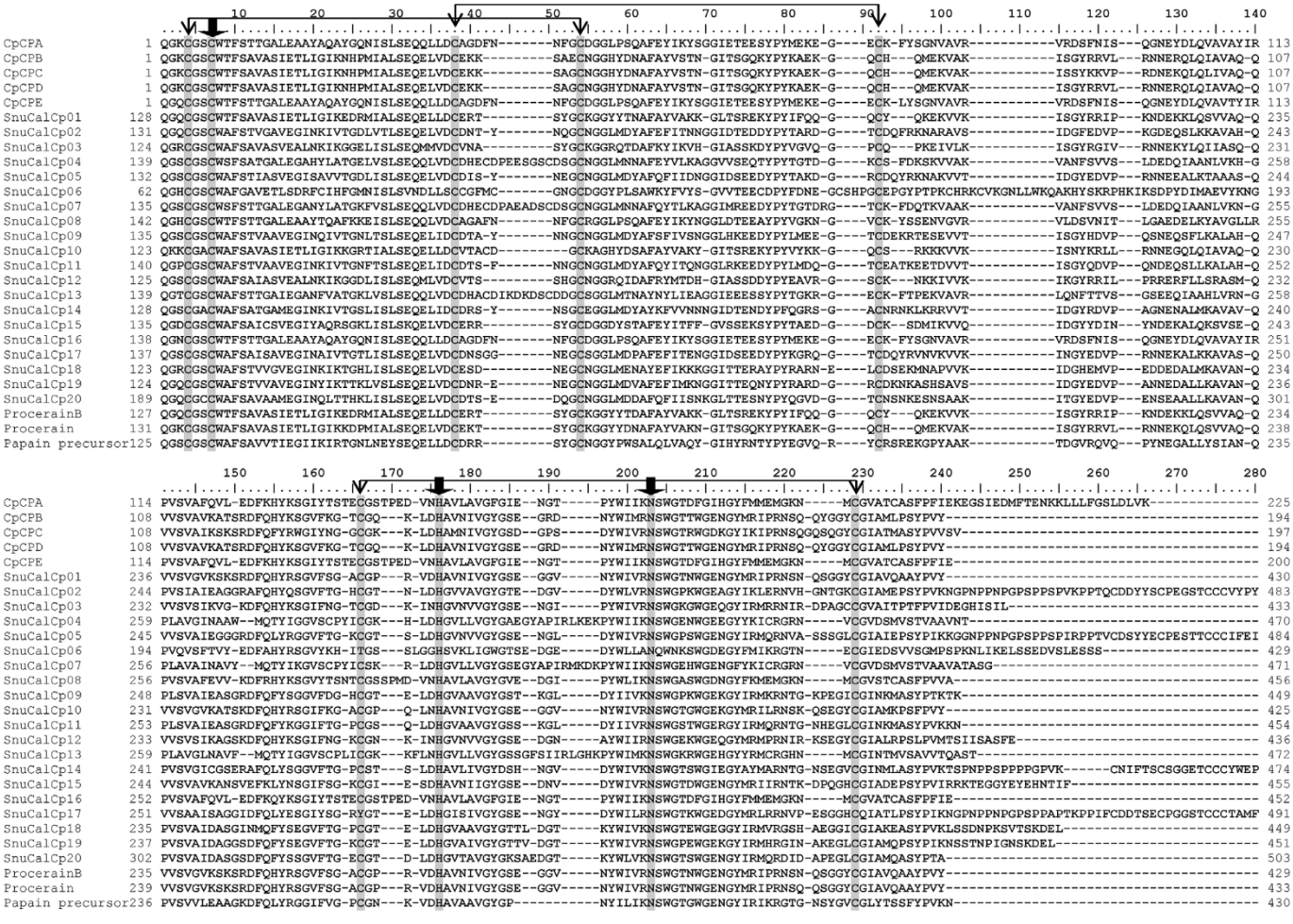

Fig. 1. Multiple amino acid sequence alignment of *C. procera* cysteine peptidases. Sequence alignment was performed with *C. procera* cysteine peptidases (CpCP A-E), (SnuCalCp 01–20), procerain B, procerain and papain. The highly conserved cysteine residues that participate in the disulfide bond formation are highlighted in gray and the conserved residues involved in the active site are indicated by vertical black arrows.

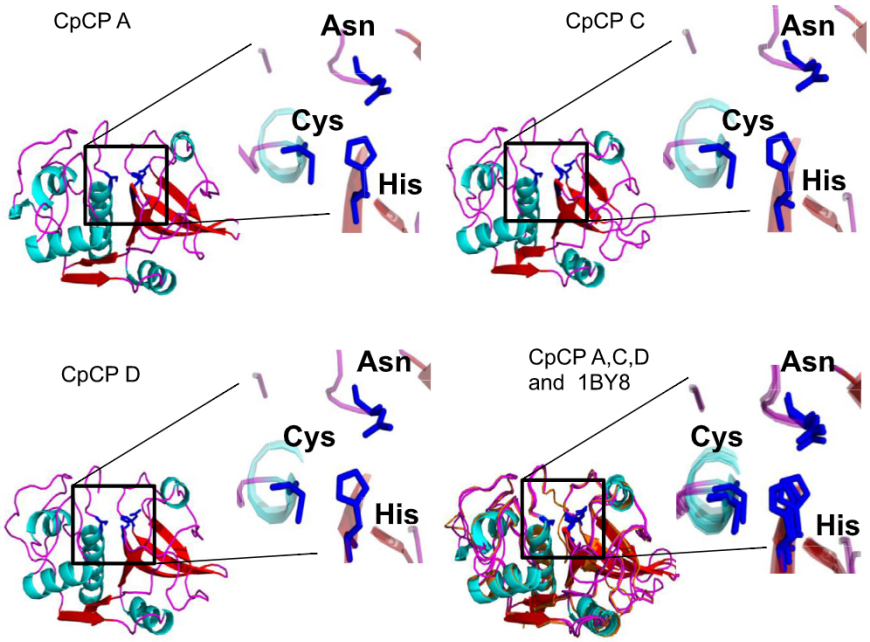

Fig. 2. Three-dimensional models of cysteine peptidases from *Calotropis procera* (CpCP A, CpCP C and CpCP D). The models were generated with the SWISS-MODEL platform and show their active sites for proteolytic activity, which are constituted by the triad Cys, Asn and His. The cysteine peptidase (PDB: 1BY8) was used as a reference.

spores, overproduction of ROS (reddish-brown precipite) was observed.

To determine whether the proteolytic activity was relevant for the antifungal effect, latex peptidases were inhibited with iodoacetamide (IAA), which is an irreversible inhibitor of cysteine peptidases, before assaying. Inhibition of fungal growth, alteration of membrane permeability (data not shown), and ROS production induced by peptidases were abolished by prior treatment of the peptidases with IAA (Fig. 7), supporting the hypothesis that the proteolytic activity fully accounts for the antifungal action.

3. Discussion

The results of 3' RACE-PCR using four degenerate forward primers yielded cDNA fragments of approximately 660–830 pb, close to the expected sizes (23 kDa) for mature cysteine peptidases from *C. procera* latex (CpCP1, CpCP2, and CpCP3) (Ramos et al., 2013). Similarly, Singh et al. (2013) cloned a 750 bp cDNA fragment from *C. procera* identified as a cysteine peptidase, then named Procerain B. Afterward, the PCR products were sequenced, and after eliminating the identical amino acid sequences of procerain, procerain B and those other 20 cysteine peptidases (SnuCalCp1-20) previously described from *C. procera* (Kwon et al., 2015), five cysteine peptidase sequences were identified, and then called CpCP A-E (Fig. 1). All sequences started with QGQ/KCGSCWTF, corresponding to the last ten amino acids in the N-terminal sequence from CpCP 1, CpCP2 and CpCP 3 (FPVPCSVDWREKGALVPIKN***QGRCGSCWAF***) (Ramos et al., 2013). As pointed out in experimental section, this sequence was chosen to design the primers because it was well conserved and matched well with other plant cysteine peptidases.

CpCP B, CpCP C, and CpCP D showed similar characteristics to procerain, whose pI was predicted to be 9.3 and molecular mass to be 23.8 kDa. In addition, they contain seven cysteine residues, among which six are involved in the formation of three disulfide bridges (Singh et al., 2013). On the other hand, CpCP A and CpCP E were acidic proteins (pI 4.0), showing eight cysteine residues and three disulfide bridges. These two enzymes were more similar to cysteine peptidase from *Nicotiana sylvestris* (Table 1). In general, all five cysteine peptidases (CpCP A-E) exhibited high biochemical similarity (molecular masses, pI, numbers of cysteine residues and disulfide bridges) with other plant cysteine peptidases (Table 1).

Cysteine peptidases hydrolyze peptide bonds using the thiol group of free cysteine residues present in active sites. The reaction usually involves a catalytic triad consisting of the thiol group of cysteine (nucleophile), the imidazolium ring of a histidine, and a third residue, usually asparagine, which orient and activate the imidazolium ring (Feijoo-Siota and Villa, 2011). This conserved triad has been found in all cysteine peptidases from *C. procera,* including CpCP A-E (Singh et al., 2013; Kwon et al., 2015). Moreover, the three-dimensional models were very close to those of other plant cysteine peptidases, exhibiting two typical domains (L and R domains), which form the "V-shaped" active site. These results indicate that the cysteine peptidases from *C. procera* have the same action mechanism (Singh et al., 2013; Kwon et al., 2015). However, some differences were found in their amino acid sequences (Fig. 1). These differences may be responsible for specific biochemical characteristics of each peptidase, such as optimum pH, V_{max}, K_m, and catalytic efficiency (Fig. 3). For instance, CpCP1, CpCP2 and CpCP3 exhibited slight differences in their optimum activity pH as well as some differences in their activities at temperatures higher than 40 °C. V_{max}, K_m, K_{cat}, and the catalytic efficiencies were also different. Other cysteine peptidases from *C. procera* latex, such as procerain and procerain B, exhibited optimum pH and temperature of 6.5–8.5 and 55–60 °C and 7.0 and 40–60 °C, respectively. How small differences in the amino acid sequences of each peptidase can influence their enzymatic kinetics is not clear and deserves further research (Dubey and Jagannadham, 2003; Singh et al., 2010; Ramos et al., 2013).

In addition to their roles in primary metabolism, some studies have attributed defensive roles to latex peptidases, mainly against insects (Konno et al., 2004; Konno, 2011; Upadhyay, 2012). For example, Konno and collaborators (2004) showed that cysteine peptidases from papaya latex were highly toxic to the larvae of generalist caterpillars, such as *Samia ricini*, *Mamestra brassicae,* and *Spodoptera litura*. On the other hand, the effects of latex cysteine peptidases on phytopathogenic fungi are poorly investigated and hence not clear. To date, only a few studies have been published describing the antifungal activity of latex cysteine peptidases (Souza et al., 2011; Ramos et al., 2014; Torres-Ossandón et al., 2019). Here, three cysteine peptidases purified from *C. procera* latex (CpCP1, CpCP2, and CpCP3) exhibited antifungal activity against two phytopathogenic fungi. Although the IC_{50} values were not

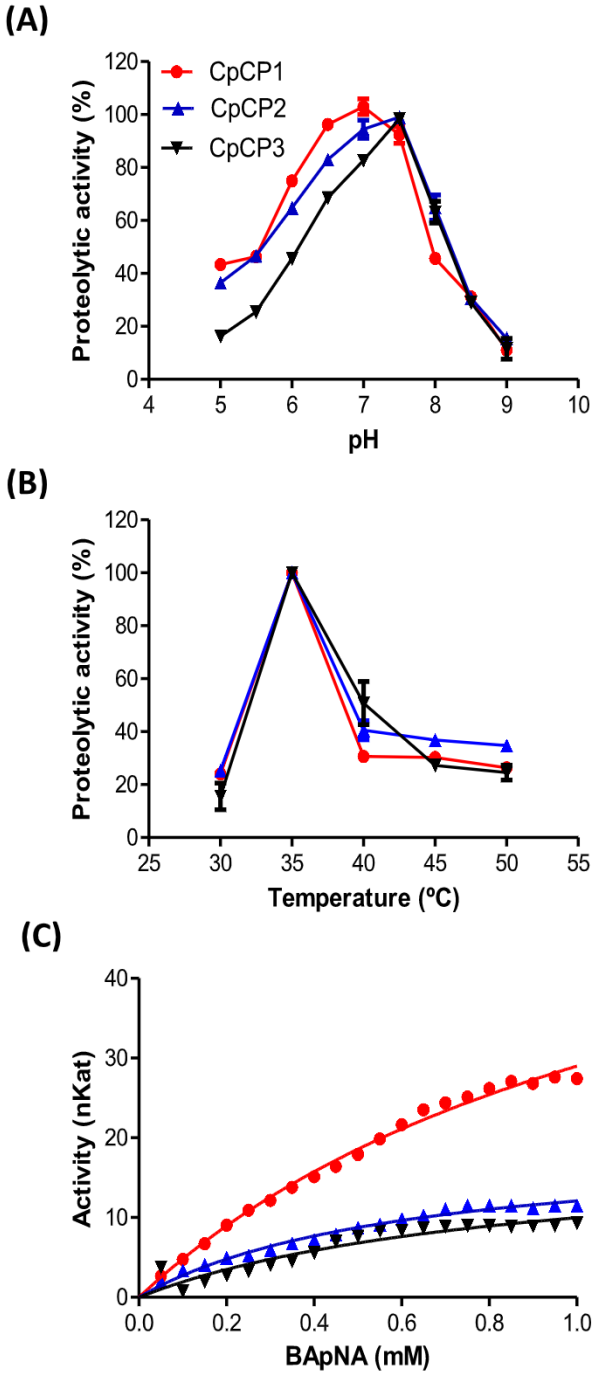

Fig. 3. Effect of pH, temperature and substrate concentration on the proteolytic activity of CpCP1, CpCP2 and CpCP3. In (A) and (B), the assays were performed using 1 mM BApNA as substrate. In B, the proteolytic activity was assayed at pH 7.0. In (C), the assays were performed using different concentrations of BApNA at pH 7.0, 35 °C, and 100 µg of each peptidase. K_m and V_{max} were determined from a nonlinear curve fit of the untransformed data using GraphPad Prism 7. The numbers used to define the kinetic parameters were best-fit estimate ± SE.

statistically different, they could indicate, at least in part, that small variations in primary structures of each peptidase may result in different biological activities or affinities upon interaction with different targets/substrates. That can be seen in Fig. 5, where CpCP1 treatment caused more extensive damage to spores than CpCP2 and CpCP3. These differences can be explained by their enzymatic kinetics (Fig. 3C). CPCP1 was more active than CpCP2 and CpCP3, although the optimum pH and temperatures were very similar. Likewise, Ramos and

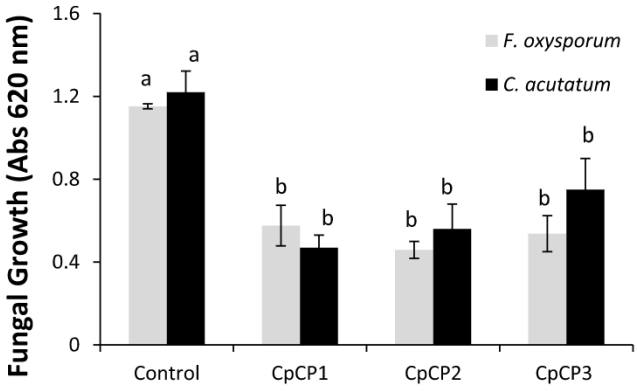

Fig. 4. Antifungal activity of three cysteine peptidases (CpCP1, CpCP2 and CpCP3) from *Calotropis procera* latex on *Fusarium oxysporum* and *Colletotrichum acutatum*. The fungal growth was measured by absorbance at 620 nm after 72 h at 27 °C. Control: 50 mM sodium phosphate buffer (pH 7.0, containing 1 mM L-Cysteine). The samples were dissolved in 50 mM sodium phosphate buffer, containing 1 mM L-cysteine, at 50 µg/mL. Different letters indicate statistical difference compared with the control ($p < 0.05$).

collaborators (2013) showed that CpCP1, CpCP2 and CpCP3 exhibited different plasma clotting activities.

Because many antifungal proteins have the ability to destroy or damage the plasma membrane, it was evaluated this damage in *F. oxysporum* spores after incubation with CpCP1, CPCP2, and CPCP3. Atomic force microscopy was chosen to evaluate the membrane damage because it is a powerful tool able to record nanostructural details of different samples, from a single protein to cells. Moreover, AFM is a nonintrusive technology that needs minimal sample preparation, avoiding metallic coating, fixation or an additional dye, and the interpretation of the results is straightforward (Braet and Taatjes, 2018). The AFM results showed that the shape and volume of fungal spores exposed to each proteolytic enzyme were significantly altered (Fig. 5), which was confirmed by uptake of propidium iodide (Fig. 6). The assays with propidium iodide also showed a massive, agglomerated, and uncommon fluorescence instead of punctual fluorescence inside the spores (Ramos et al., 2014; Oliveira et al., 2019b). Our first hypothesis for such a result was that latex cysteine peptidases caused extensive damage or formed pores in cell membranes, leading to their lysis and release of spore DNA in the medium, which in turn interacted with propidium iodide, resulting in a strong and diffuse fluorescence. Because of the membrane damage indicated by the propidium iodide assay, new experiments were performed to estimate a possible pore size caused by CpCP1, CPCP2 and CPCP3 using FITC-conjugated molecules with different molecular sizes [6000 Da (Calcein), 20,000 Da (FT-20), and 30,000 Da (FT-30)]. Interestingly, no fluorescence was detected in any of the samples. These results gave us a new hypothesis that latex peptidases do not form pores.

In general, latex cysteine peptidases are monomers, such as papain and ficin, and there are no reports that these proteins can cross the cell membrane or be inserted in the fungal plasma membrane in such a way that alters its permeability, causing cell death. On the other hand, there is one study that shows a latex cysteine peptidase forming a hexamer, which is organized as a trimer of dimers composed of a central channel (Freitas et al., 2016b). However, this unusual peptidase, named Peruvianin-I, was classified as a germin-like protein (GLP) with proteolytic activity, because its amino acid sequence and tridimensional structure are more related to GLP than to any another cysteine peptidase (Cruz et al., 2019). Interestingly, Peruvianin-I did not exhibit antifungal activity. Thus, the possible oligomerization of this protein in fungal cell membranes to form pores and then to kill the phytopathogens was discarded. The lack of antifungal activity was associated with its low

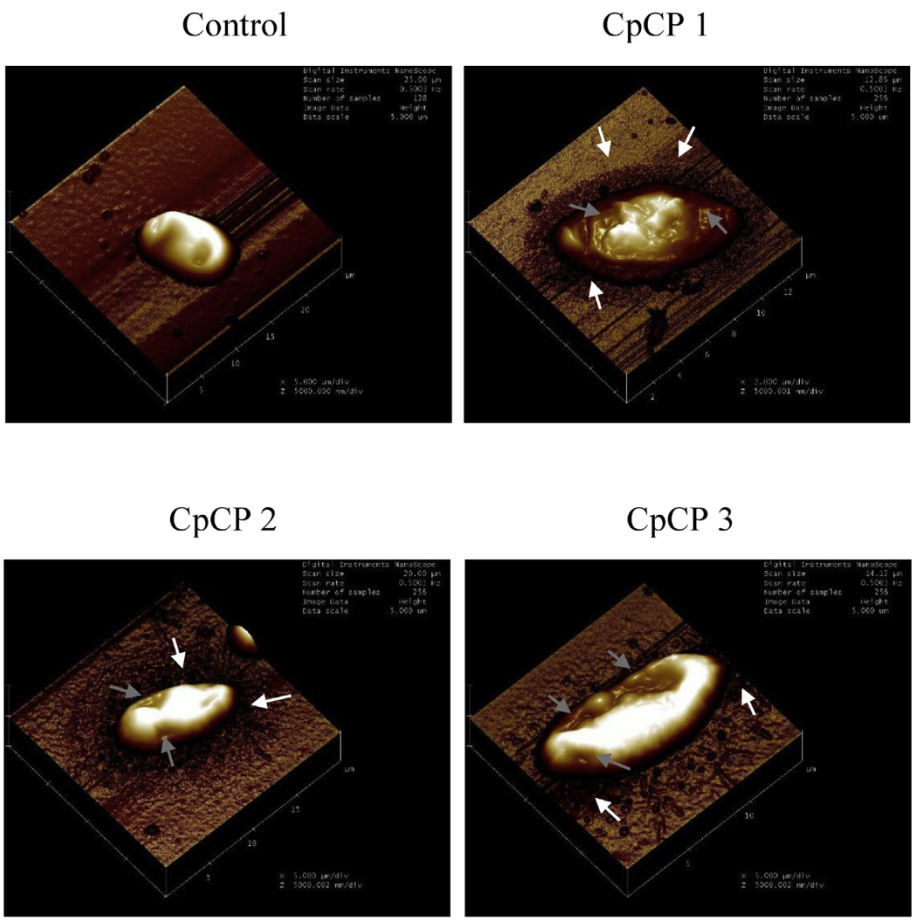

Fig. 5. Atomic force microscopic images of *Fusarium oxysporum* spores treated with the three cysteine peptidases from *Calotropis procera* (CpCP1, CpCP2 and CpCP3). The changes in the cell morphology (gray arrows) and the leakage of cellular (white arrows) content in the vicinity of the spores treated with peptidases can be observed. Peptidases (50 µg/mL) were incubated with spore suspensions for 30 min at 27 °C. Control: 50 mM sodium phosphate buffer (pH 7.0).

proteolytic activity compared with other latex cysteine peptidases (Freitas et al., 2016b). Accordingly, CpCP1, CPCP2 and CPCP3 lacking proteolytic activity lost their antifungal activities and were not able to induce any alteration in spore membrane. Similarly, a cysteine peptidase of *Vasconcellea cundinamarcencis* latex exhibited no antifungal activity after being inhibited with a specific cysteine peptidase inhibitor (Torres-Ossandón et al., 2019) or when the latex cysteine peptidase from *Cryptostegia grandiflora* was denatured, digested, or inhibited with iodoacetamide (Ramos et al., 2014). Therefore, these results support the hypothesis that the peptidases cannot be inserted in the fungal plasma membrane to alter its permeability.

Recently, it was reported that a cysteine peptidase from *V. cundinamarcencis* latex exhibited antifungal activity, provoking alterations in membrane integrity and inducing production of reactive oxygen species (ROS) (Torres-Ossandón et al., 2019), very similar to the results found here (Fig. 7). ROS can destroy essential molecules of cells, such as DNA,

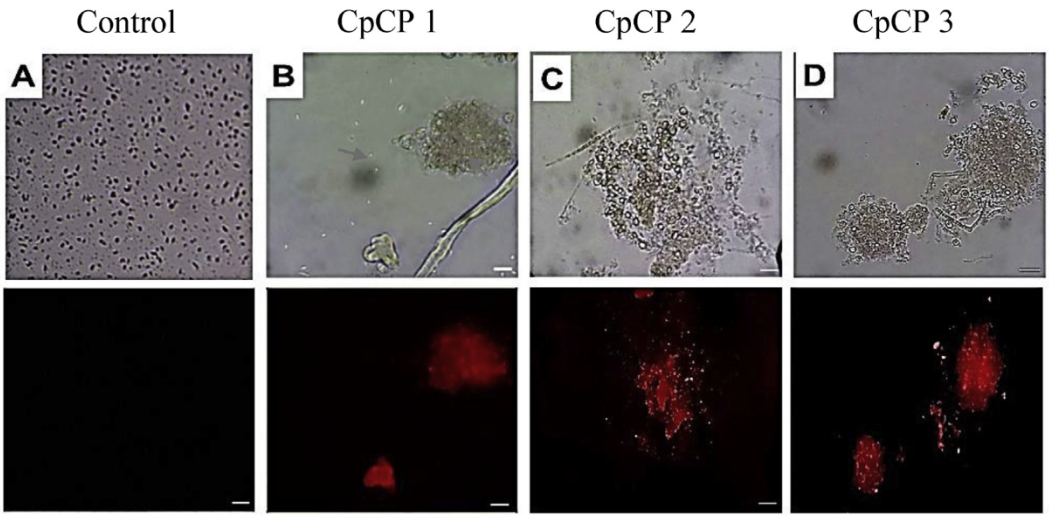

Fig. 6. Membrane permeabilization induced by cysteine peptidases from *Calotropis procera* latex in spores of *Fusarium oxysporum*. Peptidases (50 µg/mL) were incubated with spore suspensions (2×10^6 spores/mL) for 30 min at 27 °C and then the fluorescence of propidium iodide was detected using fluorescence microscopy. Bars: 5 µm. Control: 50 mM sodium phosphate buffer (pH 7.0).

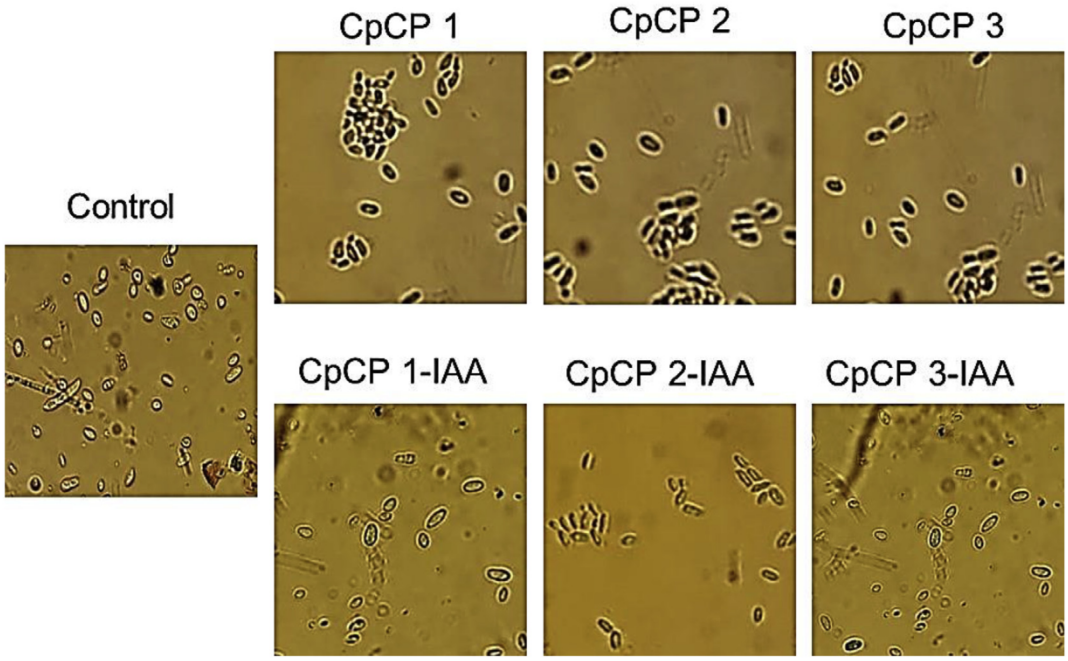

Fig. 7. Detection of ROS in spores of *F. oxysporum* after treatment with latex peptidases (CpCP1, CpCP2 and CpCP3) or inhibited with iodoacetamide (CpCP 1-IAA, CpCP 2-IAA and CpCP 3-IAA). Uptake of DAB was identified by the presence of a reddish-brown precipite. Samples (50 μg/mL) were incubated with spores for 30 min at 27 °C, pH 7.0. Control: 50 mM sodium phosphate buffer (pH 7.0). (For interpretation of the references to colour in this figure legend, the reader is referred to the Web version of this article.)

RNA, proteins, and plasma membranes, resulting in apoptosis and leakage of internal cell contents (Wang et al., 2015). However, the mechanism involved in ROS induction by peptidases is still unclear (Torres-Ossandón et al., 2019).

4. Conclusion

In this study, five undescribed cysteine peptidase genes from *Calotropis procera* were identified and characterized. Although the purified proteins showed similar tridimensional structures as other cysteine peptidases from *C. procera* latex, they showed different enzymatic kinetics. How small differences in their amino acid sequences can influence their enzymatic kinetics and biological activities, and why *C. procera* latex produces several peptidases isoforms, are unclear and warrant further research. In addition, this study brings new information for understanding the mechanisms behind the antifungal activity of latex peptidases. We hypothesized that after hydrolyzing membrane proteins, the peptidases induce the overproduction of ROS, leading to cell death. Subsequently, the membrane is destabilized, its permeability altered, and then destroyed, releasing all the intracellular content. The results reported here provide evidence that the cysteine peptidases of latex play a defensive role in plants against fungal infection.

5. Experimental

5.1. Plant material

Leaves and fresh latex of healthy plants of *Calotropis procera* (Aiton) Dryand (Apocynaceae), growing in the city of Fortaleza, Ceará, Brazil (3°44′45.9″S 38°34′21.5′W) were collected between August and September 2017 (dry season). The plant material was identified by a botanist and a plant exsiccate (no. 32,663) was deposited in the Prisco Bezerra Herbarium of Federal University of Ceará.

5.2. RNA isolation

Total RNA was isolated from young leaves of *C. procera* using the SV Total RNA Isolation kit (Promega, Madison, WI, USA), according to the manufacturer's instructions. RNA concentration was determined by measuring the absorbance at 260 nm using a NanoDrop spectrophotometer, while its integrity was evaluated by 1% agarose gel electrophoresis.

5.3. cDNA synthesis, amplification, cloning and sequencing

Total RNA samples were treated with RNase-free DNase I (E.C. 3.1.21.1) (Promega, SP, Brazil) and complementary DNA sequences (cDNAs) encoding cysteine peptidases (EC 3.4.22) were synthesized and amplified by Rapid Amplification of cDNA Ends (RACE), using the FirstChoice RLM-RACE kit (Ambion Life Technologies, CA, USA), according to the manufacturer's instructions. Briefly, poly (A)+ mRNAs were converted to cDNA using M-MLV reverse transcriptase (EC 2.7.7.49) and the 3′ RACE adapter (Table S2). First-strand cDNA products were then amplified by PCR using a gene-specific forward primer and the 3′ RACE outer primer. Four different gene-specific degenerate primers were used (Table S2), which were designed based on the N-terminal amino acid sequence of mature cysteine peptidases (CpCP1, CpCP2, and CpCP3) purified from *C. procera* (Ramos et al., 2013). To design these primers, the previously reported N-terminal sequence ($_{1}$FPVPCSVDWREKGALVPIKNQGRCGSCWAF$_{30}$) was aligned with several sequences of plant cysteine peptidases belonging to different families of the order Gentianales, in which the family Apocynaceae is classified. These multiple alignments revealed a stretch of 10 residues ($_{21}$QGRCGSCWAF$_{30}$), in which most of them were conserved in the compared sequences. Next, DNA sequences encoding the representative Gentianales proteins were aligned and codon preferences for each residue of the conserved peptide were recorded and used to design the degenerate primers. Partial cDNA fragments presumptively encoding *C. procera* cysteine peptidases were amplified by PCR and cloned in the pGEM-T Easy vector (Promega, SP, Brazil) as described by Ramos et al.

(2015). The complete sequences of cloned cDNA fragments were determined at Macrogen Inc. (Seoul, South Korea) using Sanger's dideoxy chain termination method. Removal of vectors and low-quality sequences and assembly of cDNA contigs were performed as previously described by Ramos et al. (2015).

5.4. Bioinformatic analysis

5.4.1. Sequence analysis

Editing and comparisons of cDNA and amino acid sequences were routinely performed using the BioEdit 7.2.5 software package (Hall, 1999). The translate tool on the ExPASy Proteomics Server was used to translate cDNA sequences into protein sequences (Gasteiger et al., 2003). The EMBOSS Pepstats server was used to compute the theoretical molecular mass and pI and cysteine residues (http://www.bioinformatics.nl/emboss-explorer/) (Rice et al., 2000). The DiANNA 1.1 web server was used to predict the disulfide bridges (http://clavius.bc.edu/~clotelab/DiANNA/) (Ferrè and Clote, 2006). The BLASTP was used to compare the protein query sequence against a protein sequence database at NCBI (https://blast.ncbi.nlm.nih.gov/Blast.cgi). Multiple sequence alignments of amino acids were performed using the Clustal Omega software (http://www.ebi.ac.uk/Tools/msa/clustalo/) (Sievers and Higgins, 2014). The phylogenetic tree was constructed from multiple alignments of amino acid sequences using Mega v. 7.0 (Kumar et al., 2016).

5.4.2. Molecular modeling

The protein structures were predicted by homology molecular modeling using three servers: MODELLER 9.416 (Webb and Sali, 2014); Swiss Model (https://swissmodel.expasy.org/interactive) (Biasini et al., 2014); and GalaxyWeb (http://galaxy.seoklab.org/cgi-bin/submit.cgi?type=TBM) (Shin et al., 2014). The crystal structures of different cysteine peptidases (PDB: 1BY8, 7PCK, 1IWD or 1S4V) were used to construct the models because they shared the best sequence identities with *C. procera* cysteine peptidases. The models were then analyzed using MOLPROBIT (http://molprobity.biochem.duke.edu/) (Chen et al., 2010), Verify 3D (http://services.mbi.ucla.edu/Verify_3D/) (Eisenberg et al., 1997), ERRAT (http://services.mbi.ucla.edu/ERRAT/) and ProSA (https://prosa.services.came.sbg.ac.at/prosa.php), and then were visually checked with PyMOL (http://pymol.org/).

5.5. Protein purification and identification

Purified cysteine peptidases from *C. procera* latex (CpCP1, CpCP2 and CpCP3) were obtained according to Ramos et al. (2013). The three peptidases were digested by trypsin and the resulting peptides were analyzed using a Synapt HDMS mass spectrometer (Waters, Manchester, UK) coupled to a 2D Nano UPLC-ESI system, as described by Freitas et al. (2016b). Finally, the peptides were aligned against the five cysteine peptidase cDNA sequences (CpCP A; CpCP B; CpCP C; CpCP D; CpCP E) using the Clustal Omega software (http://www.ebi.ac.uk/Tools/msa/clustalo/).

5.6. Kinetic parameters

The kinetic parameters of CpCP1, CpCP2 and CpCP3 were determined at different temperatures (30, 35, 40, 45 and 50 °C) and pH values (5.0, 5.5, 6.0, 6.5, 7.0, 7.5, 8.0, 8.5, and 9.0) using N_{α}-Benzoyl-DL-arginine *p*-nitroanilide hydrochloride (BApNA) (Sigma Aldrich, St. Louis, Missouri) as substrate, according to Baeyens-Volant et al. (2015). Hydrolysis of BApNA at the bond between the arginine and the p-nitroaniline moieties releases the chromophore p-nitroaniline, which can be measured spectrophotometrically using $\varepsilon_{410\ nm} = 8800\ M^{-1}\ cm^{-1}$.

Briefly, each test tube (total volume: 2.0 mL) contained 1 mM BApNA, 1 mM L-cysteine and 100 µL of each peptidase (1 mg/mL). After 30 min, the reaction was stopped by adding 500 µL of 50% acetic acid. One unit of activity (nkat) was defined as the amount of enzyme able to hydrolyze 1 nmoL of substrate per second. K_m (Michaelis-Menten constant) and V_{max} (maximal velocity) were determined using different concentrations of BApNA (0–1000 µM) at 35 °C, pH 7.0 and 100 µg of each peptidase from a nonlinear curve fit of the untransformed data using GraphPad Prism 7 (GraphPad Software, Inc., La Jolla, USA). K_{cat} (turnover number, $K_{cat} = V_{max}/[E]$) and K_{cat}/K_m (catalytic efficiency) were also calculated. All assays were performed in triplicate. The numbers used to define the kinetic parameters were best-fit estimate ± SE.

5.7. Antifungal assays

5.7.1. Growth inhibition

Spore suspensions of *Fusarium oxysporum* and *Colletotrichum acutatum* (2×10^5 spores/mL) were obtained in sterile water from 2-week-old cultures as described by Souza et al. (2011). CpCP 1, CpCP2, and CpCP3 were dissolved at different concentrations (10–250 µg/mL) in sterile 50 mM sodium phosphate buffer (pH 7.0, containing 1 mM L-cysteine) and the inhibition of fungal growth was evaluated by absorbance at 620 nm after 72 h (Souza et al., 2011). The concentration of cysteine peptidase able to inhibit fungal growth by 50% (IC_{50}) was obtained by absorbance compared with the control, which represented the fungal growth in the absence of peptidases (100%).

5.7.2. Mechanism of action

The action mechanism of the three cysteine peptidases (CpCP1, CpCP2 and CpCP3) was evaluated by atomic force microscopy and fluorescence using the fluorophore propidium iodide. Moreover, new assays were performed to estimate the size of the pores and oxidative stress in fungal spores. All assays were performed by incubating suspensions of *F. oxysporum* spores (2×10^4 spores/mL) for 30 min at 25 °C with 50 µg/mL (IC_{50}) of purified cysteine peptidases. Other incubation times were not tested because 30 min was the minimum time to see the effect of each peptidase on spores.

5.7.2.1. Atomic force microscopy (AFM). The effect of latex peptidases on fungal spore surfaces was determined by atomic force microscopy (AFM), as described by Ramos et al. (2015). After the incubation time, 10 µL aliquots of the spores, treated with cysteine peptidases, were placed directly on mica surfaces treated with poly-L-lysine and incubated at 25 °C for 30 min. Then, the mica was submitted to three washes with ultra-pure water to remove the excess of unabsorbed material and dried for 2 h at 25 °C in a desiccator with a vacuum. The AFM images were acquired with a Nanoscope IIIa multimode microscope using the intermittent (or tapping) mode with a rectangular TESP probe model (Bruker) having a nominal spring constant of k = 40 N/m, resonance frequency of 320 kHz, and nominal tip radius of 8 nm.

5.7.2.2. Membrane damage and ROS production. After incubation with each peptidase, the fluorophore propidium iodide was added at a final concentration of 1 µM, and after 30 min, the DNA fluorescence was measured using a fluorescence measurement system (Olympus System Microscopy) at an excitation wavelength of 480 nm and an emission wavelength of 580 nm, according to Freitas et al. (2011).

To estimate a possible size of the pores formed in the spore membrane of *F. oxysporum* induced by cysteine peptidases, the spores were incubated with different FITC-Dextrans (Sigma Aldrich, St. Louis, Missouri), according to Oliveira et al. (2019b). First, the spores were treated with each cysteine peptidase (50 µg/mL, IC_{50}) as described for the fluorescence assay. Then, the spores were incubated with FITC-dextran with size of 6000 Da (Calcein), 20,000 Da (FT20) or 30,000 Da (FT 30) for 30 min at 25 °C. Finally, the fluorescence was read using a fluorescence measurement system (Olympus System Microscope) at an excitation wavelength of 495 nm and an emission wavelength of

519 nm.

The oxidative stress caused in fungal spores after peptidase treatments was measured by the ROS production according to Oliveira et al. (2019b). Briefly, after the spores were treated with each cysteine peptidase, the samples were incubated with 100 µL of 3,3'-diaminobenzidine (DAB, 1.0 mg/mL) for 30 min at 25 °C in the dark. Then, the spores were analyzed under a light microscope (Olympus System BX60). A reddish-brown stain reaction indicated ROS production.

5.8. Inhibition of CpCP with iodoacetamide (IAA)

To determine whether the proteolytic activity was responsible for the antifungal effect, CpCP1, CpCP2, and CpCP3 were dissolved in 50 mM sodium phosphate buffer (pH 7.0), containing 1 mM L-cysteine, and incubated with 5 mM iodoacetamide (IAA, irreversible cysteine peptidase inhibitor) at 25 °C for 1 h, followed by extensive dialysis against distilled water and freeze-drying. These samples were named CpCP 1-IAA, CpCP 2-IAA, and CpCP 3-IAA and their remaining proteolytic activity was measured using azocasein as substrate (Freitas et al., 2007). Antifungal activity, membrane damage and ROS production were evaluated as described before.

5.9. Statistical analysis

All assays of antifungal activity were performed with three independent experiments and in triplicates. The results were compared by one-way analysis of variance (ANOVA), followed by the Tukey test ($p < 0.05$) using the GraphPad Prism 7 program (GraphPad Software, Inc., La Jolla, USA).

Contributions

ROS and TBG performed RNA isolation, cDNA synthesis, amplification and cloning. CDTF and CTMN performed all bioinformatic analyses. MVR, DFF, PFNS, and LPD performed the antifungal activities and JSS the atomic force microscopy assays. CDTF, MVR, PFNS and TBG contributed to data analysis, discussion and wrote the manuscript.

Declaration of competing interest

The authors confirm that the contents of this article involve no conflicts of interest.

Acknowledgments

This work was supported by grants from the following Brazilian agencies: Conselho Nacional de Desenvolvimento Científico e Tecnológico (CNPq), Coordenação de Aperfeiçoamento de Pessoal de Nível Superior (CAPES), and Fundação Cearense de Apoio ao Desenvolvimento Científico e Tecnológico (FUNCAP). This study is part of the consortium "Molecular Biotechnology of Plant Latex". We are grateful to Prof. José Tadeu Abreu de Oliveira for some antifungal assays.

Appendix A. Supplementary data

Supplementary data to this article can be found online at https://doi.org/10.1016/j.phytochem.2019.112163.

References

Avila-Ospina, L., Moison, M., Yoshimoto, K., Masclaux-Daubresse, C., 2014. Autophagy, plant senescence, and nutrient recycling. J. Exp. Bot. 65, 3799–3811.

Baeyens-Volant, D., Matagne, A., El Mahyaoui, R., Wattiez, R., Azarkan, M., 2015. A novel form of ficin from *Ficus carica* latex: purification and characterization. Phytochemistry 117, 154–167.

Biasini, M., Bienert, S., Waterhouse, A., Arnold, K., Studer, G., Schmidt, T., Kiefer, F., Gallo-Cassarino, T., Bertoni, M., Bordoli, L., Schwede, T., 2014. SWISS-MODEL: modelling protein tertiary and quaternary structure using evolutionary information. Nucleic Acids Res. 42, W252–W258.

Braet, F., Taatjes, D.J., 2018. Foreword to the special issue on applications of atomic force microscopy in cell biology. Semin. Cell Dev. Biol. 73, 1–3.

Chen, V.B., Arendall, W.B., Headd, J.J., Keedy, D.A., Immormino, R.M., Kapral, G.J., Murray, L.W., Richardson, J.S., Richardson, D.C., 2010. MolProbity: all-atom structure validation for macromolecular crystallography. Acta Crystallogr. 66, 12–21.

Chen, W., Shao, J., Ye, M., Yu, K., Bednarek, S.Y., Duan, X., Guo, W., 2017. Blueberry VcLON 2, a peroxisomal LON protease, is involved in abiotic stress tolerance. Environ. Exp. Bot. 134, 1–11.

Cruz, W.T., Bezerra, E.H.S., Grangeiro, T.B., Lopes, J.L.S., Silva, M.Z.R., Ramos, M.V., Rocha, B.A.M., Oliveira, J.S., Freitas, D.C., Freitas, C.D.T., 2019. Structural and enzymatic characterization of Peruvianin-I, the first germin-like protein with proteolytic activity. Int. J. Biol. Macromol. 126, 1167–1176.

Daneva, A., Gao, Z., Van Durme, M., Nowack, M.K., 2016. Functions and regulation of programmed cell death in plant development. Annu. Rev. Cell Dev. Biol. 32, 441–468.

Domsalla, A., Melzig, M.F., 2008. Occurrence and properties of proteases in plant latices. Planta Med. 74, 699–711.

Dubey, V.K., Jagannadham, M.V., 2003. Procerain, a stable cysteine protease from the latex of *Calotropis procera*. Phytochemistry 62, 1057–1071.

Eisenberg, D., Lüthy, R., Bowie, J.U., 1997. VERIFY3D: assessment of protein models with three-dimensional profiles. Methods Enzymol. 277, 396–404.

Feijoo-Siota, L., Villa, T.G., 2011. Native and biotechnologically engineered plant proteases with industrial applications. Food Bioprocess Technol. 4, 1066–1088.

Ferrè, F., Clote, P., 2006. DiANNA 1.1: an extension of the DiANNA web server for ternary cysteine classification. Nucleic Acids Res. 34, W182–W185.

Figueiredo, A., Monteiro, F., Sebastiana, M., 2014. Subtilisin-like proteases in plant–pathogen recognition and immune priming: a perspective. Front. Plant Sci. 5, 739.

Freitas, C.D.T., Oliveira, J.S., Miranda, M.R.A., Macedo, N.M.R., Sales, M.P., Villas-Boas, L.A., Ramos, M.V., 2007. Enzymatic activities and protein profile of latex from *Calotropis procera*. Plant Physiol. Biochem. 45, 781–789.

Freitas, C.D.T., Souza, D.P., Araújo, E.S., Cavalheiro, M.G., Oliveira, L.S., Ramos, M.V., 2010. Anti-oxidative and proteolytic activities and protein profile of laticifer cells of *Cryptostegia grandiflora, Plumeria rubra* and *Euphorbia tirucalli*. Braz. J. Plant Physiol. 22, 11–22.

Freitas, C.D.T., Lopes, J.L.S., Beltramini, L.M., Oliveira, R.S.B., Oliveira, J.T.A., Ramos, M.V., 2011. Osmotin from *Calotropis procera* latex: new insights into structure and antifungal properties. Biochim. Biophys. Acta Biomembr. 1808, 2501–2507.

Freitas, C.D.T., Leite, H.B., Oliveira, J.P.B., Amaral, J.L., Egito, A.S., Vairo-Cavalli, S., Lobo, M.D.P., Monterio-Moreira, A.C.O., Ramos, M.V., 2016a. Insights into milk-clotting activity of latex peptidases from *Calotropis procera* and *Cryptostegia grandiflora*. Food Res. Int. 87, 50–59.

Freitas, C.D.T., Cruz, W.T., Silva, M.Z.R., Vasconcelos, I.M., Moreno, F.B.M.B., Moreira, R.A., Monteiro-Moreira, A.C.O., Alencar, L.M.R., Sousa, J.S., Rocha, B.A.M., Ramos, M.V., 2016b. Proteomic analysis and purification of an unusual germin-like protein with proteolytic activity in the latex of *Thevetia peruviana*. Planta 243, 1115–1128.

Gasteiger, E., Gattiker, A., Hoogland, C., Ivanyi, I., Appel, R.D., Bairoch, A., 2003. ExPASy: the proteomics server for in-depth protein knowledge and analysis. Nucleic Acids Res. 31, 3784–3788.

Hall, T.A., 1999. BioEdit: a user-friendly biological sequence alignment editor and analysis program for Windows 95/98/NT. Nucleic Acids Symp. Ser. 41, 95–98.

Hou, S., Jamieson, P., He, P., 2018. The cloak, dagger, and shield: proteases in plant-pathogen interactions. Biochem. J. 475, 2491–2509.

Konno, K., Hirayama, C., Nakamura, M., Tateishi, K., Tamura, Y., Hattori, M., Kohno, K., 2004. Papain protects papaya trees from herbivorous insects: role of cysteine proteases in latex. Plant J. 37, 370–378.

Konno, K., 2011. Plant latex and other exudates as plant defense systems: roles of various defense chemicals and proteins contained therein. Phytochemistry 72, 1510–1530.

Kumar, S., Stecher, G., Tamura, K., 2016. MEGA7: molecular evolutionary genetics analysis version 7.0 for bigger datasets. Mol. Biol. Evol. 33, 1870–1874.

Kwon, C.W., Park, K.M., Kang, B.C., Kweon, D.H., 2015. Cysteine protease profiles of the medicinal plant *Calotropis procera* R.Br. revealed by de novo transcriptome analysis. PLoS One 10, e0119328.

Lopéz, L.M.I., Viana, C.A., Errasti, M.E., Garro, M.L., Martegani, J.E., Mazzilli, G.A., Freitas, C.D.T., Araújo, I.M.S., Silva, R.O., Ramos, M.V., 2017. Latex peptidases of *Calotropis procera* for dehairing of leather as an alternative to environmentally toxic sodium sulfide treatment. Bioproc. Biosyst. Eng. 40, 1391–1398.

Lu, H., Chandrasek, B., Oeljeklaus, J., Misas-Villamil, J.C., Wang, Z., Shindo, T., Bogyo, M., Kaiser, M., van der Hoorn, R.A.L., 2015. Subfamily-specific fluorescent probes for cysteine proteases display dynamic protease activities during seed germination. Plant Physiol. 168, 1462–1475.

Meyer, M., Huttenlocher, F., Cedzich, A., Procopio, S., Stroeder, J., Pau-Roblot, C., Lequart-Pillon, M., Pelloux, J., Stintzi, A., Schaller, A., 2016. The subtilisin-like protease SBT3 contributes to insect resistance in tomato. J. Exp. Bot. 67, 4325–4338.

Nelson, C.J., Millar, A.H., 2015. Protein turnover in plant biology. Nat. Plants 15017, 1–7.

Oliveira, J.P.B., Candreva, A.M., Rizzo, G., Ramos, M.V., Oliveira, J.S., Oliveira, H.D., Ary, M.B., Docena, G., Freitas, C.D.T., 2019a. Allergenicity reduction of cow's milk proteins using latex peptidases. Food Chem. 284, 245–253.

Oliveira, J.T.A., Souza, P.F.N., Vasconcelos, I.M., Dias, L.P., Martins, T.F., van Tilburg, M.F., Guedes, M.I.F., Sousa, D.O.B., 2019b. *Mo*-CBP$_3$-PepI, *Mo*-CBP$_3$-PepII, and *Mo*-CBP$_3$-PepIII are synthetic antimicrobial peptides active against human pathogens by stimulating ROS generation and increasing plasma membrane. Biochimie 157, 10–21.

Ramos, M.V., Viana, C.A., Silva, A.F.B., Freitas, C.D.T., Figueiredo, I.S.T., Oliveira, R.S.B., Alencar, N.M.N., Lima-Filho, J.V.M., Kumar, V.L., 2012. Proteins derived from latex

of *C. procera* maintain coagulation homeostasis in septic mice and exhibit thrombin- and plasmin-like activities. Naunyn-Schmiedeberg's Arch. Pharmacol. 385, 455–463.
Ramos, M.V., Araújo, E.S., Jucá, T.L., Monteiro-Moreira, A.C.O., Vasconcelos, I.M., Moreira, R.A., Viana, C.A., Beltramini, L.M., Pereira, D.A., Moreno, F.B., 2013. New insights into the complex mixture of latex cysteine peptidases in *Calotropis procera*. Int. J. Biol. Macromol. 58, 211–219.
Ramos, M.V., Souza, D.P., Gomes, M.T.R., Freitas, C.D.T., Carvalho, C.P.S., Junior, P.A.V.R., Salas, C.E., 2014. A phytopathogenic cysteine peptidase from latex of wild rubber vine *Cryptostegia grandiflora*. Protein J. 33, 199–209.
Ramos, M.V., Oliveira, R.S.B., Pereira, H.M., Moreno, F.B.M.B., Lobo, M.D.P., Rebelo, L.M., Brandão-Neto, J., Sousa, J.S., Monteiro-Moreira, A.C.O., Freitas, C.D.T., Grangeiro, T.B., 2015. Crystal structure of an antifungal osmotin-like protein from *Calotropis procera* and its effects on *Fusarium solani* spores, as revealed by atomic force microscopy: insights into the mechanism of action. Phytochemistry 119, 5–18.
Ramos, M.V., Alencar, N.M.N., Oliveira, R.S.B., Freitas, L.B.N., Aragão, K.S., Andrade, T.A.M., Frade, M.A.C., Brito, G.A.C., Figueiredo, I.S.T., 2016. Wound healing modulation by a latex protein-containing polyvinyl alcohol biomembrane. Naunyn-Schmiedeberg's Arch. Pharmacol. 389, 747–756.
Ramos, M.V., Demarco, D., Souza, I.C.C., Freitas, C.D.T., 2019. Laticifers, latex, and their role in plant defense. Trends Plant Sci. 24, 553–567.
Rice, P., Longden, I., Bleasby, A., 2000. EMBOSS: the European molecular biology open software suite. Trends Genet. 16, 276–277.
Shin, W.H., Lee, G.R., Heo, L., Lee, H., Seok, C., 2014. Prediction of protein structure and interaction by GALAXY protein modeling programs. Bio Design 2, 1–11.
Sievers, F., Higgins, D.G., 2014. Clustal Omega, accurate alignment of very large numbers of sequences. Methods Mol. Biol. 1079, 105–116.
Singh, A.N., Shukla, A.K., Jagannadham, M.V., Dubey, V.K., 2010. Purification of a novel cysteine protease, procerain B, from *Calotropis procera* with distinct characteristics compared to procerain. Process Biochem. 45, 399–406.
Singh, A.N., Yadav, P., Dubey, V.K., 2013. cDNA cloning and molecular modeling of Procerain B, a novel cysteine endopeptidase isolated from *Calotropis procera*. PLoS One 8, e59806.
Souza, D.P., Freitas, C.D.T., Pereira, D.A., Nogueira, F.C., Silva, F.D., Salas, C.E., Ramos, M.V., 2011. Laticifer proteins play a defensive role against hemibiotrophic and necrotrophic phytopathogens. Planta 234, 183–193.
Torres-Ossandón, M.J., Vega-Gálvez, A., Salas, C.E., Rubio, J., Silva-Moreno, E., Castilho, L., 2019. Antifungal activity of proteolytic fraction (P1G10) from (*Vasconcellea cundinamarcensis*) latex inhibit cell growth and cell wall integrity in *Botrytis cinerea*. Int. J. Food Microbiol. 289, 7–16.
Upadhyay, R.K., 2012. Plant latex: its toxicity and defense against herbivorous insects: a review. Int. J. Curr. Res. 4, 5–10.
van der Hoorn, R.A.L., 2008. Plant proteases: from phenotypes to molecular mechanisms. Annu. Rev. Plant Biol. 59, 191–223.
van Wijk, K.J., 2015. Protein maturation and proteolysis in plant plastids, mitochondria, and peroxisomes. Annu. Rev. Plant Biol. 66, 75–111.
Wang, K., Dang, W., Xie, J., Zhu, R., Sun, M., Jia, F., Zhao, Y., An, X., Qiu, S., Li, X., Ma, Z., Yan, W., Wang, R., 2015. Antimicrobial peptide protonectin disturbs the membrane integrity and induces ROS production in yeast cells. Biochim. Biophys. Acta 1848, 2365–2373.
Webb, B., Sali, A., 2014. Protein structure modeling with MODELLER. Methods Mol. Biol. 1137, 1–15.
Zare, H., Moosavi-Movahedi, A.A., Salami, M., Mirzaei, M., Saboury, A.A., Sheibani, N., 2013. Purification and autolysis of the ficin isoforms from fig (*Ficus carica* cv Sabz) latex. Phytochemistry 87, 16–22.
Zhang, D., Liu, D., Lv, X., Wang, Y., Xun, Z., Liu, Z., Li, Z., Lu, H., 2014. The cysteine protease CEP1, a key executor involved in tapetal programmed cell death, regulates pollen development in Arabidopsis. Plant Cell 26, 2939–2961.